Microscale laser shock imprinting of micro-molds with different sizes and shapes

Haifeng Yang[1, 2, 3], Kun Liu[1*], Hao Liu[1]

[1]School of Mechatronic Engineering, China University of Mining and Technology,
Xuzhou, 221116, China

[2]Jiangsu Key Laboratory of Mine Mechanical and Electrical Equipment,
China University of Mining and Technology, Xuzhou, 221116, China

[3]School of Industrial Engineering, Purdue University,
West Lafayette, Indiana 47907, USA

[*]Corresponding author: liuk1995@163.com

There are higher requirements for microstructures and high-precision components in microelectronics, photonics, sensors, optoelectronics and medical devices. For changing the traditional manufacturing methods with cumbersome process and complex equipment, researchers put forward a laser shock forming technique which can contribute to the metal forming with high precision and efficiency in recent years. So far, the laser shock forming needed high pulse energy and high energy. In this paper, nanosecond laser with high frequency and low pulse energy was adopted to make possible the aluminum foil forming on the copper micro-molds with different sizes and shapes. The deformations of aluminum foil were measured by SEM, optical profiler and AFM. Also, the deformation laws were analyzed by comparing imprinting results under different micro-molds. Lastly, stress distribution and deformation process of aluminum foil was investigated by numerical simulations.

Keywords: laser shock, imprinting, micro-mold, deformation depth, numerical simulation.

1. Introduction

In the modern manufacture industry, microminiaturization has become a trend which was setting for high precision and microsize products in many fields, just like MEMS, photology, medicine, *etc*. But traditional manufacturing methods of metal microforming have some limitations, such as complex manufacturing equipment, poor precision and low efficiency. Besides, traditional methods are hard to meet the sample's requirements that are high strength and difficult formation. It is necessary to explore a new method to solve the current problems of the micro-metal formation. In recent years, researchers have put forward a kind of laser shock microforming method, which can

improve the mechanical properties of deformed metal [1–3]. The products made by the method were adopted not only in MEMS [4, 5], but also in optoelectronics technologies [6, 7], medical equipment [8] and sensing application [9, 10]. Considering that the laser processing technique has many advantages [11–13], researchers have carried out extensive studies about the laser shock microforming. CHAO ZHENG *et al*. put forward microscale laser bulge forming which was a high strain rate microforming method using high-amplitude shock wave pressure, and they investigated the deformed copper's (thickness of 30 μm) residual stress distribution with different laser energy [14]. JI LI *et al*. studied the forming limit and fracture of thin foil by using microscale laser dynamic forming with laser pulse energy 850 mJ [15]. XIAO WANG *et al*. analyzed the thickness distribution at the cross-section of micro-channel after laser indirect shock micro-embossing, and used strain states during micro-embossing to interpret the variation in thickness distribution [16]. HUIXIA LIU *et al*. investigated the influences of laser energy and defocussing distance on surface roughness and deformation degree with molds size in the range from 250 μm to 1 mm [4, 17]. HUIXIA LIU *et al*. also put forward the laser shock micro-punching, which mainly focused on the cutting contour feature and blanking morphology [18]. NAGARAJAN *et al*. investigated the thinning behavior of copper foil induced by flexible-pad laser shock forming [19]. HUANG GAO *et al*. reported a low-cost, high-throughput method that can create three-dimensional crystalline metallic structures as small as 10 nanometers with an ultrasmooth surface at ambient conditions [20]. Most of these studies used laser with high pulse energy, which increased energy consumption and reduced safety. In addition, these researches focused on the unique forming methods of microstructures, without the comparison between different structures and different scales.

This paper presents a laser shock imprinting method, which adopts the nanosecond laser with low pulse energy and high pulse frequency. This method can realize the large-area microstructure forming. Meanwhile, the micro-molds can recycle and reuse, which can improve efficiency and utilization ratio. On the one hand, this paper investigates the imprinting results while micro-molds have the same shape and multiple sizes. On the other hand, we investigate the relationship between metal deformation and micro-molds shape by comparing the imprinting results of micro-molds with the same size and multiple shapes. At last, the stress distribution and metal deformation progress are further analyzed by numerical simulation. Through the comprehensive analysis, we summarize the forming mechanism of the microscale laser shock imprinting using micro-molds with different sizes and shapes.

2. Experiments

2.1. Imprinting methods

Figure 1 shows the schematic of laser shock imprinting using micro-molds. An ultraviolet laser (DSH-355-10) operated at 355 nm wavelength and 10 ns pulse width served as the exposure source, which had high frequency (range from 1 Hz to 150 kHz) and low pulse
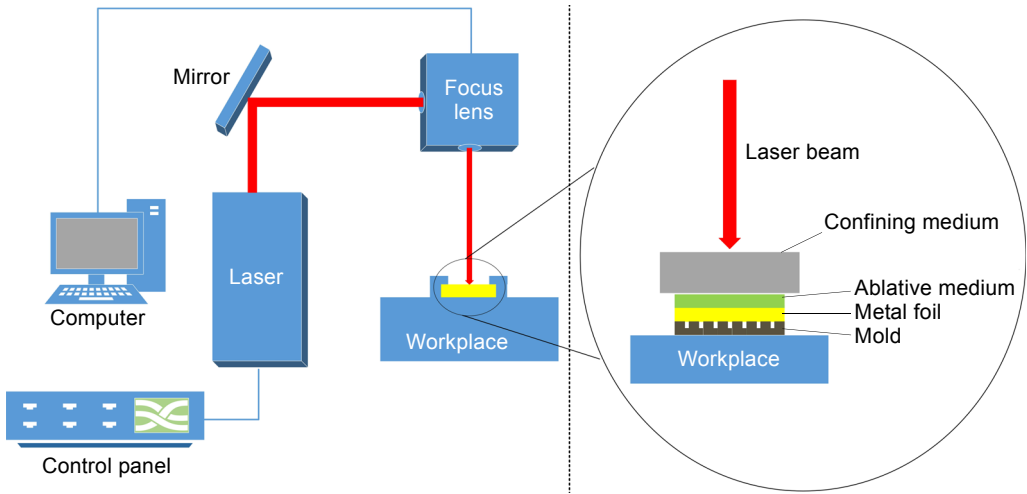
Fig. 1. Schematic of laser shock imprinting.

energy (maximum is 1.5 mJ). In the experiments, the laser beam was focused and scanned on the metal foil surface by a focus lens, which was controlled by the MarkingMate software in the computer. As shown in inset of Fig. 1, there were confining medium, ablative medium, metal foil, and micro-molds on the workplace. The focused laser beam shot on the ablative medium with small focus area during a very short time. Then, the ablative medium converted to plasma after absorbing a lot of laser energy. Under the restraint of confining medium, plasma shock wave gradually expanded down, and exported into metal foil. When the pressure exceeded the yield strength of the metal, the plastic deformation of metal foil was induced, and finally the shape of the micro-molds was replicated to the metal foil.

2.2. Experiment processes

As confining medium, K9 glass of 2 mm thickness was used to constraint a plasma shock wave. Because of its wide application and good mechanical properties, two layers of aluminum foil with 13 μm thickness were used as ablative medium and metal foil, respectively. In the process of experiment, we need to ensure that the layers were fitted closely. We used a laser with pulse energy (109 μJ), wavelength 355 nm and pulse frequency (1000 Hz) to irradiate an ablation coating layer. The simplified formula was used to calculate the laser intensity I_0, expressed as

$$I_0 = \frac{4\alpha E}{\pi d^2 \tau} \tag{1}$$

where E is the pulse energy, α is the laser absorption coefficient of material (take $\alpha = 1$), d stands for laser spot diameter ($d = 20$ μm) and τ is the pulse width ($\tau = 10$ ns). By
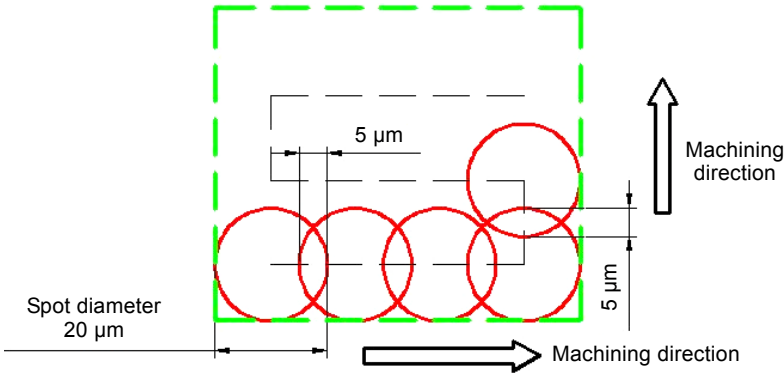
Fig. 2. Schematic of laser spot overlapping rate.

calculation, the laser intensity I_0 is about 3.5 GW/cm^2. In addition, the laser spot overlapping rate η, deciding the laser pulse impact distribution on the sample, can be indicated as

$$\eta = \frac{\varDelta}{d} \times 100\% \tag{2}$$

where $\varDelta$ is the overlapping length between the two laser spots. By using computer software to control the movement of laser spots, the experiment is realizing overlapping laser shock imprinting. The spot movement rate is 15 mm/s, the machining line spacing is 15 μm and the experimental pulse frequency is 1000 Hz. So the laser overlapping rate η was 25%, which was shown in Fig. 2.

   The copper micro-molds with multiple mesh sizes (200#, 400#, 1000#, and 2000#) and mesh shapes (grating, square hole, and round hole) were used. Figure 3 shows the SEM images of micro-molds with different shapes and Fig. 4 shows the SEM image of unprocessed aluminum surface. The research aim is to analyze the influence of different micro-molds on the microscale laser shock imprinting results. After imprinting,
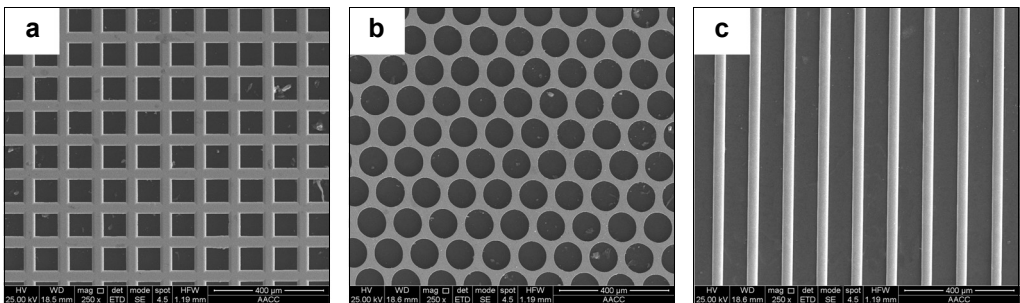

Fig. 3. The SEM images of micro-molds with different shapes: square hole (**a**), round hole (**b**), grating (**c**).
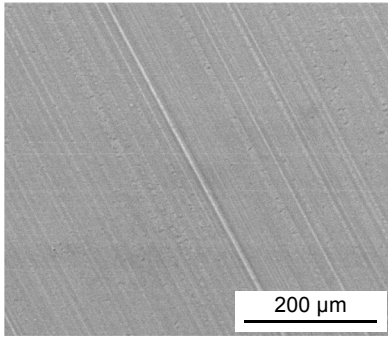
Fig. 4. The SEM image of unprocessed aluminum surface.

SEM (Quanta 250), AFM (CSPM5500, Benyuan Nano-Instrument, China) and an optical profiler (DVM5000, Leica, Germany) were used to measure the outline and depth of deformed aluminum foil.

2.3. Numerical simulations

ABAQUS software was used to analyze the metal's transient plastic deformation induced by microscale laser shock imprinting. During the laser shock imprinting process, after absorbing laser energy, the ablative medium produces plasma explosion and transfers plasma shock pressure to the surface of aluminum foil, which results in the plastic deformation. This process can be regarded as an isothermal process that takes no account of the temperature impact on the experimental results. In order to describe the relationship between stress, deformation process and pressure during the laser shock imprinting, the Johnson–Cook stain sensitive plasticity model was used, which can be expressed as follows [21]:

$$\delta = (A + B\varepsilon^n)\left(1 + C\ln\frac{\dot{\varepsilon}}{\dot{\varepsilon}_0}\right) \tag{3}$$

where ε is the plastic strain, $\dot{\varepsilon}$ is the plastic strain rate, and $\dot{\varepsilon}_0$ is the reference strain rate, A, B, C, n and m are material constants. The specific value parameters in this model of pure aluminum are listed in the Table.

Laser shock imprinting results were determined by the shock wave pressure, which depended on the laser parameters. So in the numerical simulation process, the shock wave was regarded as pressure that changed over time and directly loaded on the alu-

T a b l e. The specific value parameters in Johnson–Cook model of pure aluminum.

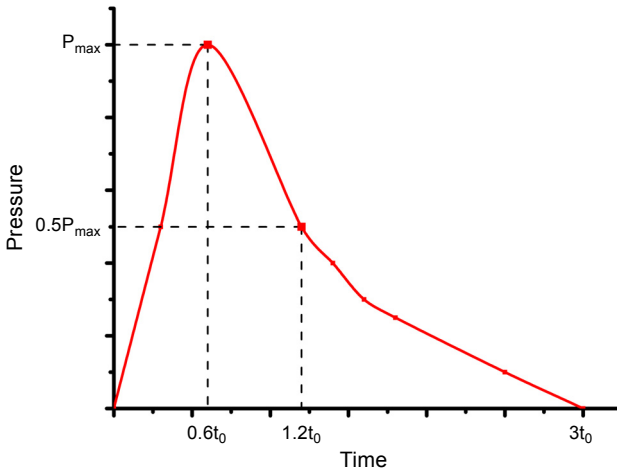| A [MPa]	B [MPa]	C	n	m	$\dot{\varepsilon}_0$
256	426	0.015	0.34	1.4	1.0

Fig. 5. The curve of shock pressure changing with the time.

minum foil surface. Due to the influence of the confining medium, the time of shock wave effecting on metal surface increases greatly, and this is three times of laser pulse width. Figure 5 shows the curve of shock pressure changing with the time (t_0 is the laser pulse width). The peak pressure is expressed as follows [22, 23]:

$$P_{\max} = 0.01\left(\frac{\alpha}{2\alpha + 3}\right)^{0.5} Z^{0.5} I_0^{0.5} \qquad (4)$$

where I_0 is the laser power density, α is the internal energy transformation factor ($\alpha = 0.1$), Z is the shock impedance between the confining medium (K9 glass) and the ablative medium (aluminum foil), where $2/Z = 1/Z_1 + 1/Z_2$, and Z_1, Z_2 is the shock impedance of confining medium and ablative medium, respectively.

3. Results and discussions

3.1. Microscale laser shock imprinting with different square hole sizes

To investigate the size effect, four kinds of sizes of copper micro-molds with square holes were chosen in the experiments. As shown in Fig. 6**a**, the size of a square hole was determined by the side size. Figure 6**b** shows its specific values of different micro-molds. With the mesh size increasing, the side size of micro-molds decreased. Figure 6**c** shows the 200# copper micro-mold measured by an optical profiler. It can be seen that the depth of the hole was approximately 37 μm.

In the laser shock imprinting process, the laser with high frequency and low pulse energy, after passing through the confining medium, is directly shot on the ablative medium (upper aluminum foil layer). Then, the ablative medium absorbs a large amount of laser energy, vaporizes and forms high pressure plasma. Under the effect of confining medium, the plasma expands down and acts on the forming metal (lower aluminum
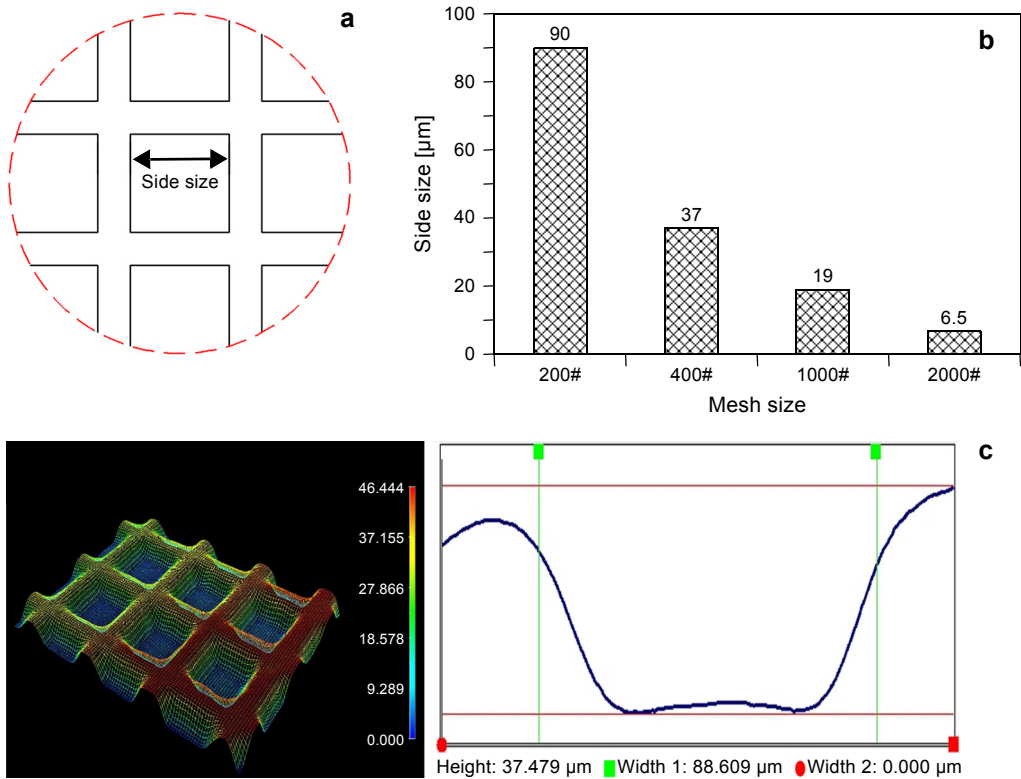
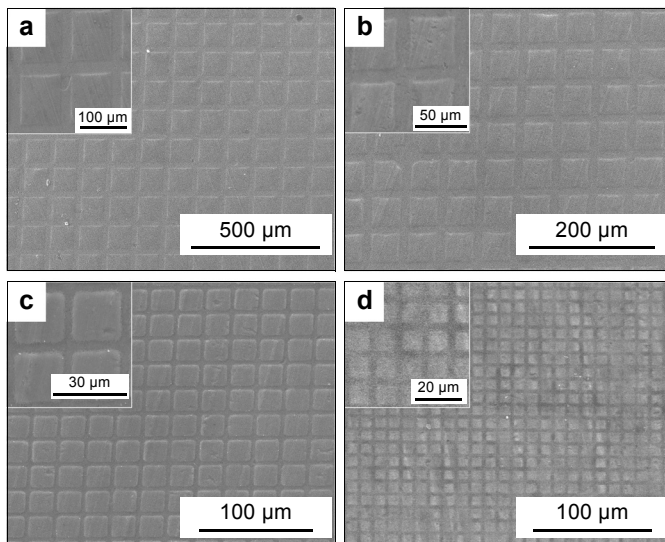Fig. 6. The size of different mesh size micro-molds (see text for explanation).

Fig. 7. SEM images of the deformed aluminum foils with different mesh sizes: 200# (**a**), 400# (**b**), 1000# (**c**), and 2000# (**d**).

foil layer). When the shock pressure exceeds the yield strength of the metal, the forming metal layer exhibits plastic deformation according to the mold shape. Figure 7 shows SEM images of the deformed aluminum foils with different mesh sizes induced by laser shock imprinting. It can be seen that micro-molds were replicated precisely and completely, including corners of square holes for four kinds of mesh sizes.

After laser shock imprinting, an optical profiler was used to measure the deformation depth of aluminum foil. For imprinting results on 2000# micro-mold, the deformation depth was not accurately measured by the optical profiler so that we adopted AFM. Figure 8**a** shows 3D profile of deformed aluminum foil on 400# micro-molds and the inset shows a dimensional section curve in deformed aluminum foil. It is concluded that the average deformation depth was about 3.5 μm. Figure 8**b** shows the 3D profile and section curve of the imprinting results on 2000# micro-molds obtained by AFM;

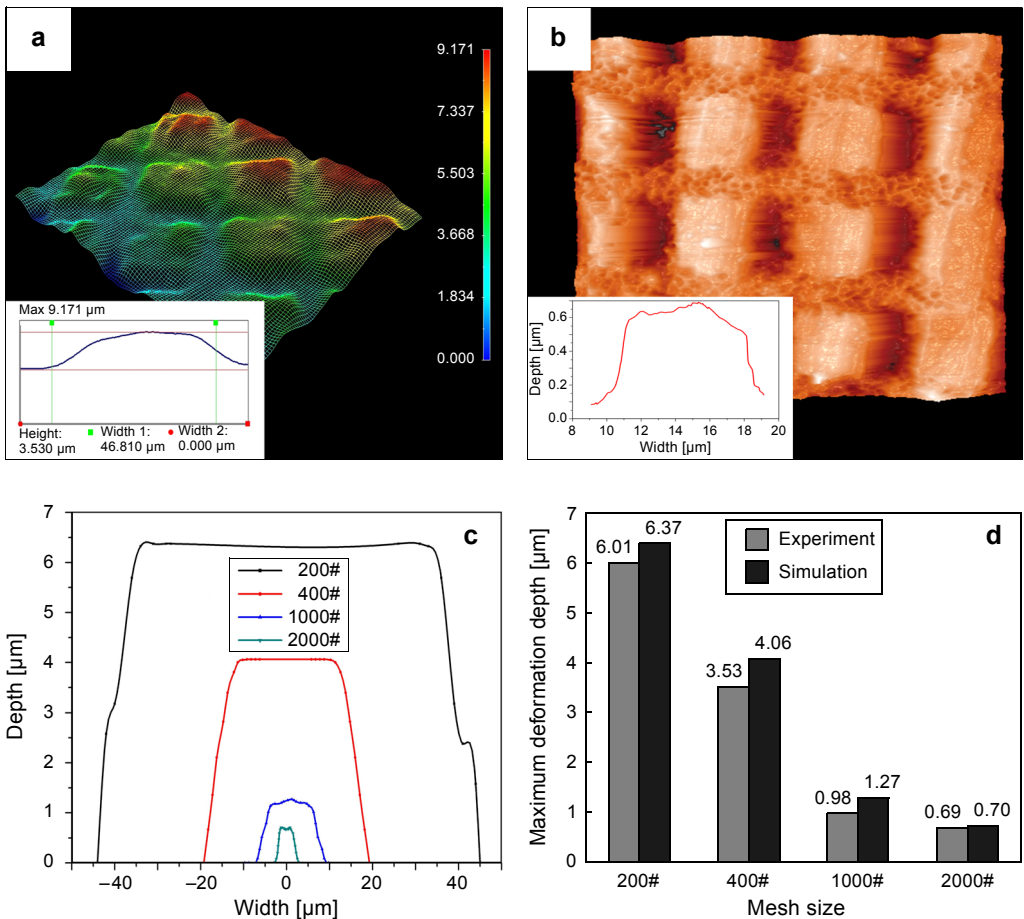Fig. 8. Forming depth of deformed aluminum foils with different mesh size (see text for explanation).

its average deformation depth was about 0.69 μm, which was far less than that of the imprinting results on 400# micro-molds. Figure 8**c** shows the simulation results of section profile curve for four kinds of mesh sizes after laser shock imprinting. Admittedly, the friction force between the micro-mold edge and aluminum foil prevents the occurrence of deformation; the deformation depth in micro-molds edge was smaller than that of the center. Nevertheless, it can be concluded that the side and bottom of square holes for four kinds of mesh sizes have very good replication results. However, there were different deformation depths for those mesh sizes. The larger the mesh size was, the deeper the deformation, which were consistent with our experiment results. Figure 8**d** shows the comparison between simulation and experiment results in terms of aluminum foil's maximum deformation depths for four kinds of mesh sizes. The side size of the square hole reduces with the increase of the mesh size. Therefore, the deformation depths of the aluminum foil reduced with the increase of the micro-molds mesh size. Firstly, the edge of the square hole in micro-mold prevents plastic deformation of aluminum foil and the smaller size of the square hole makes greater inhibition. Secondly, the thickness of aluminum also has an impact on the deformation depth. When the micro-molds are 1000# or 2000#, the thickness of aluminum foil (13 μm) is close to or greater than the side size of the square hole so that the extrusion produced by deformation would affect its further plastic deformation. Thirdly, during the plastic deformation, the high friction between the micro-mold and the metal causes a retardation of plastic flow. Stronger metals or smaller feature sizes would require higher shock pressures, and consequently higher strain rate, to trigger the superplastic flow [20]. Therefore, in the case of constant laser energy, the decrease of the side size of square hole would result in the smaller deformation degree.

In addition, the material size-scale effect is the main reason for the difference in imprinting results. In the case of ultra-high strain rate deformation, micrometer-scale metal can show different properties, such as mechanical, electrical, optical and magnetic, caused by internal dislocation avalanches. When the size of the micro-mold is small, ultra-high strain rate deformation of aluminum foil leads to different yield strengths and generates different imprinting results [24, 25].

Figure 9 shows the simulated stress distribution of deformed aluminum foil on micro-molds with different mesh sizes. The stress distribution of deformed aluminum foil was similar. It was found that the stress mainly concentrated in the corner of the deformation area. Because of the influence of the micro-molds' edge, the deformation degree in the corner of micro-molds was maximum at the moment of laser shock, so the stress concentrated relatively.

Figure 10 shows the aluminum foil's deformation process on 2000# micro-mold. The period of shock wave exerted on the aluminum foil surface is three times of the laser pulse width t_0. The maximum shock pressure appeared at $0.6t_0$ and then weakened gradually. It can be seen that the aluminum foil took large deformation before $1.2t_0$ and then its deformation speed gradually slowed down.
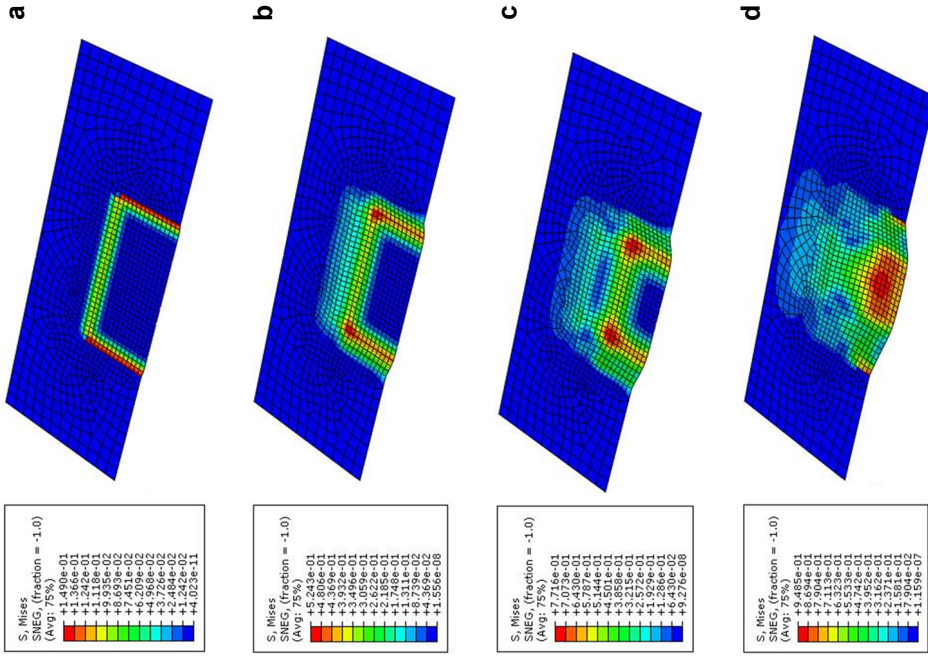
Fig. 10. Deformation process of deformed aluminum foil with 2000# mesh size micro-molds: $0.6t_0$ (**a**), $1.2t_0$ (**b**), $1.8t_0$ (**c**), and $3t_0$ (**d**).
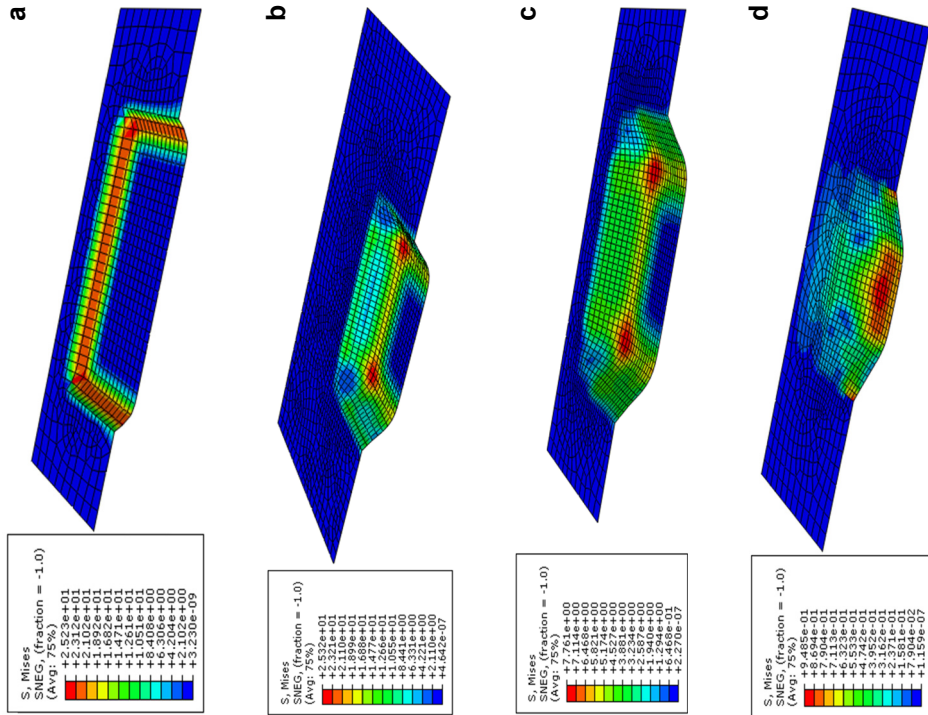

Fig. 9. Stress distribution of deformed aluminum foil with different mesh size: 200# (**a**), 400# (**b**), 1000# (**c**), and 2000# (**d**).

3.2. Microscale laser shock imprinting with different micro-mold shapes

Three kinds of copper micro-molds (grating, square hole, and round hole) with 200# were chosen to investigate some shape elements (like corner, circle and line) influence the microscale laser shock imprinting results. SEM images of different micro-molds were shown in Fig. 3. Figures 11**a** and 11**b** show the size marking of micro-molds and
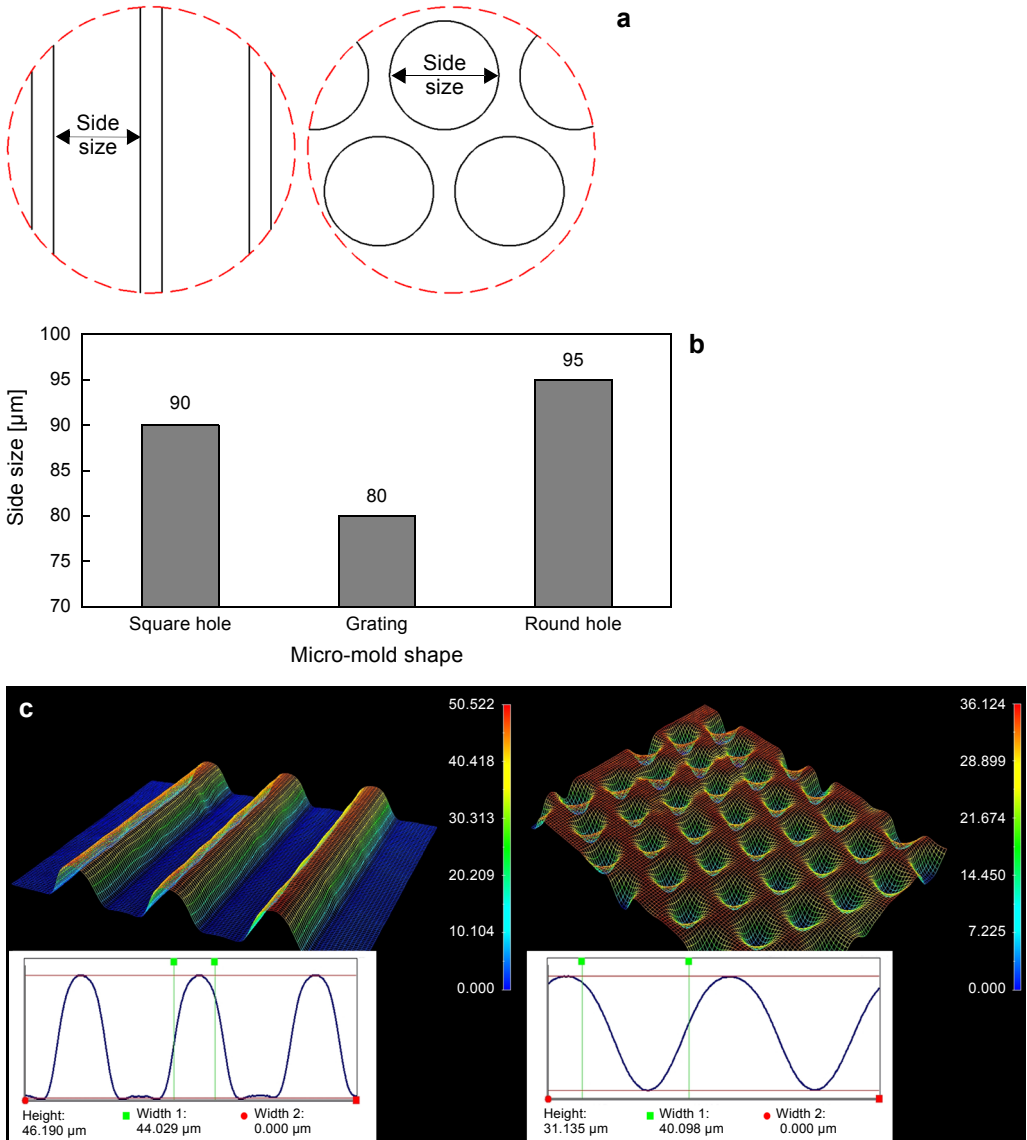
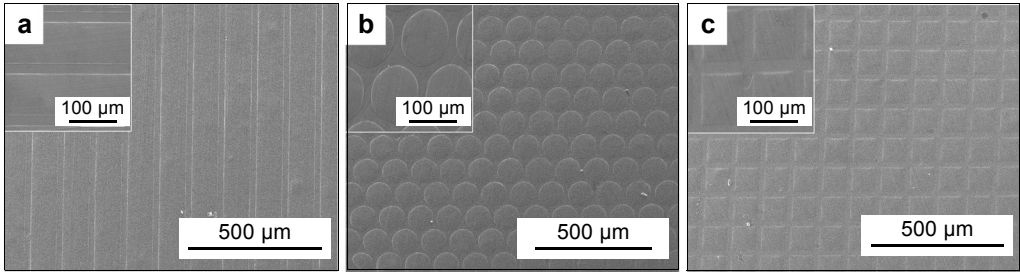Fig. 11. The size of different shape micro-molds (see text for explanation).

Fig. 12. SEM images of the deformed aluminum foils with different shape: grating (**a**), round hole (**b**), and square hole (**c**).

the side size's specific value of the micro-mold with 200#, respectively. The 3D profile and section curve of different micro-molds were shown in Fig. 11**c**.

After microscale laser shock imprinting, three kinds of deformed aluminum foils (grating, square hole, and round hole) were shown in Fig. 12. It was clear to see that no matter what was the shape (the corner, circle, or line in micro-molds), aluminum foil could replicate micro-molds accurately. Optical profiler was used to measure the deformed aluminum foil profile, section curve, and to get the specific value of the
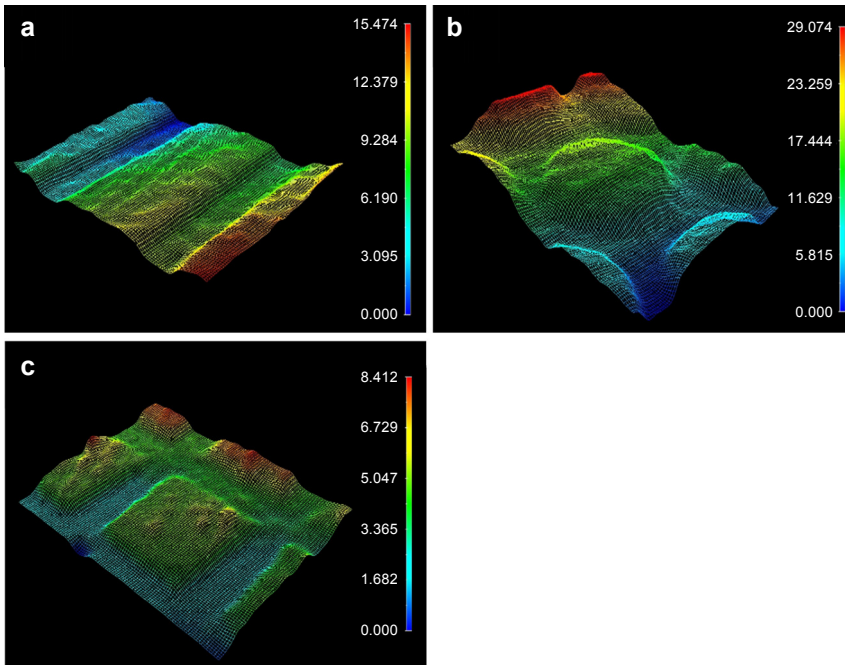

Fig. 13. 3D profile of deformed aluminum foils with different shape: grating (**a**), round hole (**b**), and square hole (**c**).
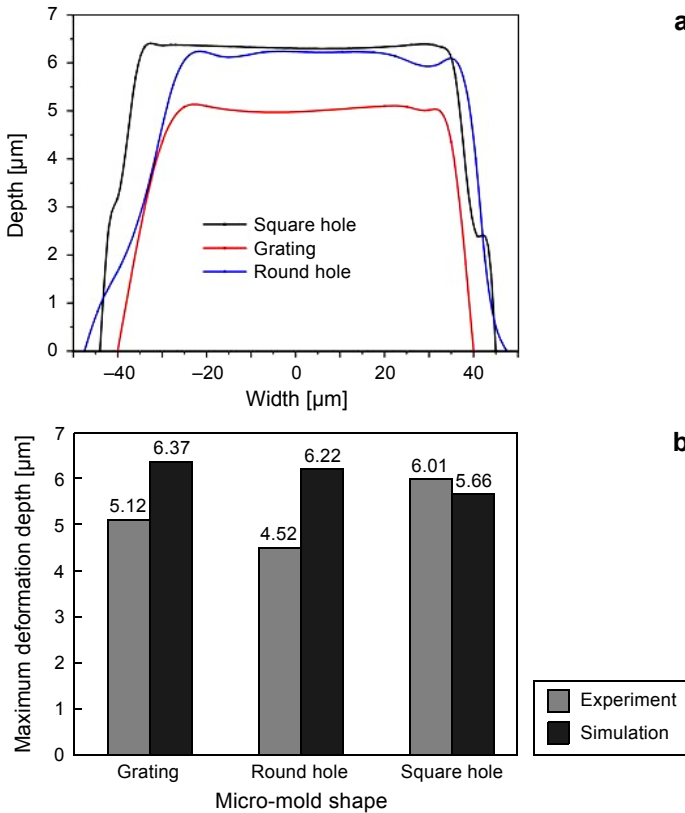
Fig. 14. Forming depth of deformed aluminum foils with different shape (see text for explanation).

deformation depth. Figure 13 shows the 3D profile of deformed aluminum foil under different micro-mold shapes.

Based on the simulation results, we can find that the aluminum foil formed plastic deformation and accurately replicated the shapes of different micro-molds. Figure 14**a** shows the section profile curve of deformed aluminum foil with different micro-molds shapes. Figure 14**b** shows the comparison between simulation and experiment results of maximum deformation depth. Micro-molds with the same mesh sizes and different shapes have small effects on the aluminum foil's deformation depth. Small differences in edge friction resistances and the effect of aluminum thickness can be attributed to the similar deformation depth. Besides, with the same scale of ultra-high strain rate deformation, the mechanical properties of aluminum foil are similar so that imprinting results have not much difference. Therefore, it can be concluded that microscale laser shock imprinting has the ability to replicate the multiple shapes of micro-molds and the shape of micro-molds has little effect on the aluminum foil's deformation depth. Figure 15 shows simulated stress distribution for micro-molds with different shapes.
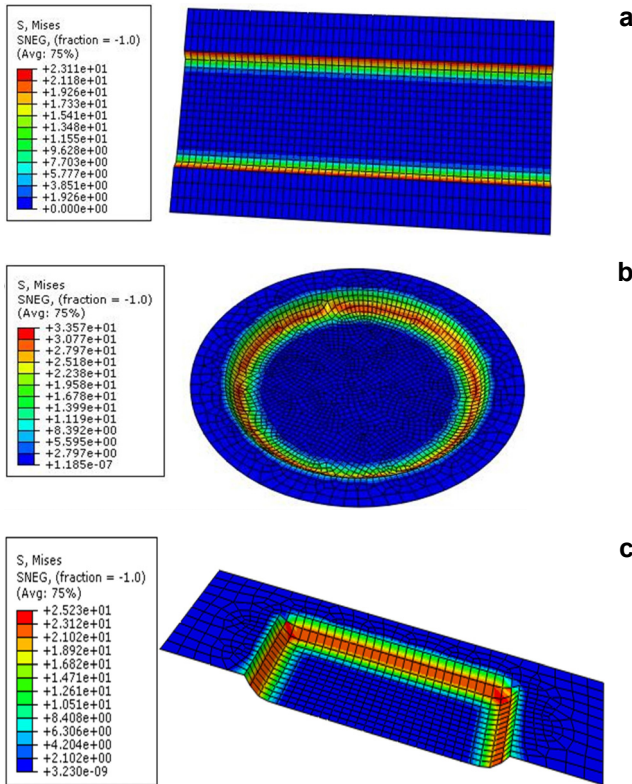
Fig. 15. Stress distribution of deformed aluminum foil with different shape: grating (**a**), round hole (**b**), and square hole (**c**).

The maximum stress also mainly concentrated in the corner of the deformation area and the stress distributions for multiple shape micro-molds had small differences.

4. Conclusions

In this paper, a nanosecond laser with high frequency and low pulse energy was adopted for microscale laser shock imprinting. Combined with the experiment and ABAQUS numerical simulation results, some conclusions, including deformation depth, stress distribution and imprinting progress for micro-molds with multiple shapes and sizes, could be drawn from the paper.

The deformation depth of laser shock imprinting results decreased as the micro-molds side size reduced. After the analysis, the friction force between the micro-molds and aluminum foil, the side size of the square hole and the thickness of aluminum foil were key factors determining the deformation depth. In addition, a material size-scale effect was the main reason for the difference in imprinting results with different size micro-molds. In the microscale laser shock imprinting process, there is little discrepancy in

the deformation degree with different micro-mold shapes. So microscale laser shock imprinting had the ability to replicate the multiple shapes of micro-molds accurately and the shape of micro-molds had little effect on the aluminum foil's deformation depth. Besides, numerical simulation results were also found and the stress mainly concentrated in the corner of the deformation region. Thus, this processing method could be efficiently used in manufacturing a large-area and diversified microstructure on metallic foil by changing mold types and laser parameters.

References

[1] CHENG G.J., PIRZADA D., ZHOU MING, *Microstructure and mechanical property characterizations of metal foil after microscale laser dynamic forming*, Journal of Applied Physics 101(6), 2007, article ID 063108.

[2] OCAÑA J.L., MORALES M., PORRO J.A., GARCÍA-BALLESTEROS J.J., CORREA C., *Laser shock microforming of thin metal sheets with ns lasers*, Physics Procedia 12, 2011, pp. 201–206.

[3] CUNJIANG YU, HUANG GAO, HONGYU YU, HANQING JIANG, CHENG G.J., *Laser dynamic forming of functional materials laminated composites on patterned three-dimensional surfaces with applications on flexible microelectromechanical systems*, Applied Physics Letters 95(9), 2009, article ID 091108.

[4] HUIXIA LIU, ZONGBAO SHEN, XIAO WANG, HEJUN WANG, MAOKE TAO, *Micromould based laser shock embossing of thin metal sheets for MEMS applications*, Applied Surface Science 256(14), 2010, pp. 4687–4691.

[5] ZONGBAO SHEN, CHUNXING GU, HUIXIA LIU, XIAO WANG, YANG HU, *Fabricating three-dimensional array features on metallic foil surface using overlapping laser shock embossing*, Optics and Lasers in Engineering 51(8), 2013, pp. 973–977.

[6] ECHTERMEYER T.J., BRITNELL L., JASNOS P.K., LOMBARDO A., GORBACHEV R.V., GRIGORENKO A.N., GEIM A.K., FERRARI A.C., NOVOSELOV K.S., *Strong plasmonic enhancement of photovoltage in graphene*, Nature Communications 2, 2011, p. 458.

[7] SCHULLER J.A., BARNARD E.S., WENSHAN CAI, YOUNG CHUL JUN, WHITE J.S., BRONGERSMA M.L., *Plasmonics for extreme light concentration and manipulation*, Nature Materials 9(3), 2010, pp. 193–204.

[8] NINGGANG SHEN, PENCE C.N., BOWERS R., YIN YU, HONGTAO DING, STANFORD C.M., OZBOLAT I.T., *Surface micro-scale patterning for biomedical implant material of pure titanium via high energy pulse laser peening*, ASME 2014 International Manufacturing Science and Engineering Conference, 2014, article ID V002T02A099.

[9] SEUNGHYUN LEE, PRASHANT KUMAR, YAOWU HU, CHENG G.J., IRUDAYARAJ J., *Graphene laminated gold bipyramids as sensitive detection platforms for antibiotic molecules*, Chemical Communications 51(85), 2015, pp. 15494–15497.

[10] CHUANG QIAN, CHAO NI, WENXUAN YU, WENGANG WU, HAIYANG MAO, YIFEI WANG, JUN XU, *Highly -ordered, 3D petal-like array for surface-enhanced Raman scattering*, Small 7(13), 2011, pp. 1801–1806.

[11] JIAXIANG MAN, HAIFENG YANG, YANQING WANG, CHENG YAN, SHANQING ZHANG, *Nanotribological properties of nanotextured Ni-Co coating surface measured with AFM colloidal probe technique*, Journal of Laser Micro/Nanoengineering **12**(1), 2017, pp. 16–21.

[12] HAIFENG YANG, HAIDONG HE, ENLAN ZHAO, JINBIN HAO, JIGUO QIAN, WEI TANG, HUA ZHU, *Electronic-controlling nanotribological behavior of textured silicon surfaces fabricated by laser interference lithography*, Laser Physics Letters 11(10), 2014, article ID 105901.

[13] HAIFENG YANG, TIANCHI CHEN, JIGUO QIAN, JING HAN, HAIDONG HE, LONGPENG ZHOU, ENLAN ZHAO, WEI TANG, HUA ZHU, *Friction-reducing micro/nanoprotrusions on electrodeposited Ni-Co alloy coating surface fabricated by laser direct writing*, Bulletin of Materials Science 38(1), 2015, pp. 173–181.

[14] CHAO ZHENG, SHENG SUN, ZHONG JI, WEI WANG, *Effect of laser energy on the deformation behavior in microscale laser bulge forming*, Applied Surface Science 257(5), 2010, pp. 1589–1595.

[15] JI LI, HUANG GAO, CHENG G.J., *Forming limit and fracture mode of microscale laser dynamic forming*, Journal of Manufacturing Science and Engineering 132(6), 2010, article ID 061005.

[16] XIAO WANG, ZONGBAO SHEN, CHUNXING GU, DI ZHANG, YUXUAN GU, HUIXIA LIU, *Laser indirect shock micro-embossing of commercially pure copper and titanium sheet*, Optics and Lasers in Engineering 56, 2014, pp. 74–82.

[17] ZONGBAO SHEN, HUIXIA LIU, XIAO WANG, HEJUN WANG, *Micromold-based laser shock embossing of metallic foil: fabrication of large-area three-dimensional microchannel networks*, Materials and Manufacturing Processes 26(9), 2011, pp. 1126–1129.

[18] HUIXIA LIU, MENGMENG LU, XIAO WANG, ZONGBAO SHEN, CHUNXING GU, YUXUAN GU, *Micro-punching of aluminum foil by laser dynamic flexible punching process*, International Journal of Material Forming 8(2), 2015, pp. 183–196.

[19] NAGARAJAN B., CASTAGNE S., ZHONGKE WANG, *Investigation of copper foil thinning behavior by flexible-pad laser shock forming*, Key Engineering Materials 535–536, 2013, pp. 306–309.

[20] HUANG GAO, YAOWU HU, YI XUAN, JI LI, YINGLING YANG, MARTINEZ R.V., CHUNYU LI, JIAN LUO, MINGHAO QI, CHENG G.J., *Large-scale nanoshaping of ultrasmooth 3D crystalline metallic structures*, Science 346(6215), 2014, pp. 1352–1356.

[21] YAOWU HU, PRASHANT KUMAR, RONG XU, KEJIE ZHAO, CHENG G.J., *Ultrafast direct fabrication of flexible substrate-supported designer plasmonic nanoarrays*, Nanoscale 8(1), 2016, pp. 172–182.

[22] FABBRO R., FOURNIER J., BALLARD P., DEVAUX D., VIRMONT J., *Physical study of laser-produced plasma in confined geometry*, Journal of Applied Physics 68(2), 1990, pp. 775–784.

[23] PEYRE P., FABBRO R., *Laser shock processing: a review of the physics and applications*, Optical and Quantum Electronics 27(12), 1995, pp. 1213–1229.

[24] UCHIC M.D., DIMIDUK D.M., FLORANDO J.N., NIX W.D., *Sample dimensions influence strength and crystal plasticity*, Science 305(5686), 2004, pp. 986–989.

[25] CSIKOR F.F., MOTZ C., WEYGAND D., ZAISER M., ZAPPERI S., *Dislocation avalanches, strain bursts, and the problem of plastic forming at the micrometer scale*, Science 318(5848), 2007, pp. 251–254.